CHALLENGES IN EUROPEAN AEROSPACE
5TH CEAS AIR & SPACE CONFERENCE

CEAS

Active Flow Control Applied at the Engine-Wing Junction

Sebastian Fricke
previously at DLR (German Aerospace Center)
Research Engineer
Lilienthalplatz 7, Braunschweig, Germany
Sebastian.Fricke@dlr.de

Vlad Ciobaca (Research Engineer, DLR, Braunschweig), Anna Kröhnert (Research Engineer, DLR, Braunschweig), Jochen Wild (Research Engineer, DLR, Braunschweig), Olivier Blesbois (Research Engineer, Airbus Operations Ltd., Filton)

ABSTRACT

The integration of UHBR (Ultra High Bypass Ratio) engines mounted under backward swept wings may lead at low speed to local flow separations on the wing suction side in the wake of the nacelle. These local flow separations can trigger the total wing stall which degrades the total aircraft performance. This paper presents a numerical study of AFC (active flow control) applied at the engine-wing junction of a generic full scale wind tunnel model to suppress the local flow separations. The AFC method is based on the principle of fluidic actuation and assembles a pulsed blowing with a 180° phase shift between the neighboring nozzles. Its working principle is the production of vortices that enhance the mixing of the boundary layer and the free stream flow. The free stream flow in the wake of the nacelle is compromised due to the wakes of local flow separations and longitudinal vortices such as the strake vortex. The computation results show that pulsed blowing is capable of suppressing the local separations. It is shown that a certain blowing velocity exists that is required for the suppression of the nacelle-wake separation. Additionally the influence of the pulse frequency was analyzed with a parameter study. It was shown that the local flow separations were suppressed by both low and high pulse frequencies.

1 INTRODUCTION

The use of UHBR (Ultra High Bypass Ratio) engines is currently one of the most promising approaches for the further increase of the efficiency of classical transport aircraft configurations (see Guynn et al. [1]). However their integration also compromises the aerodynamic efficiency of airliners with engines mounted under backward swept wings. The close coupling of the large nacelles and the wing prevents the mounting of leading edge high lift devices such as slats, Krueger flaps or droop noses over a large part of the wing in the area of the engine-wing junction. During past research (see Rudnik [2], Neitzke et al. [3], v. Geyr et al. [4]) it was shown that for high angles of attack local flow separation regions are emerging on the wing suction side downstream of the engine nacelle, which are called nacelle-wake separation (also illustrated in Figure 1). This geometry triggers complex flow phenomena emerging at the engine-wing junction, such as the interaction of nacelle vortices with the flow around the wing. The nacelle-wake separation can trigger the total wing stall at low inflow speeds and hence reduce the maximum achievable lift (see also Figure 2) which is a major parameter for the sizing of the high lift system and hence overall aircraft performance (see also van Dam [5]). For the smaller engine nacelles of current airliners the application of nacelle strakes to suppress or attenuate the influence of the nacelle-wake separation was successfully embraced by almost all transport aircraft manufacturers for underwing mounted configurations. Nacelle strakes are small triangular or delta shaped panel sheets applied on the nacelle which induces a longditudinal vortex which supports the mixing of the flow downstream of the slat cutout and enhance the maximum lift of common passenger aircraft. It is however believed, that the

use of nacelle strakes will not be sufficient for the integration of the larger UHBR nacelles (see Meyer et al. [6]). Within the European project AFLoNext [7] (Active Flow - Loads & Noise control on next generation wing) the use of AFC (active flow control) for the suppression of the flow separation is studied with high-fidelity numerical simulations and a wind tunnel experiment with a full scale generic 2.5D high-lift configuration of a engine-wing junction. The AFC can increase the kinetic energy of the boundary layer downstream of the slat cutout which can suppress the nacelle-wake separation. First results of the author's computational studies for flow control on this configuration were presented in Fricke et al. [8]. The tackled AFC methods were a constant and a pulsed blowing through slits located at the slat cutout. The results for the constant blowing showed a significant reduction of the nacelle-wake separation. The larger the blowing velocity the larger the angle of attack for which the local flow recirculation occurred. Increments in the order on 3° were realized with blowing with constant velocity of the actuators. The pulsed blowing however showed a low effect on the size of the nacelle-wake separation. The reason was found to be the large velocity deficit in the wake of a flow separation area located directly on the engine nacelle. This unwelcome flow topology was positioned inboard of the nacelle and located upstream of the actuators. It led to a flow of low energetic fluid directly over the actuators which jam the working principle of the pulsed blowing, based on the mixing of the boundary layer with the high energetic free stream flow (see Greenblatt [9]). It is believed that a significant improvement could be to use a clever nacelle strake vortex to increase the energy of the free stream flow over the actuators. This paper presents the results of the high-fidelity unsteady numerical simulations of an upgraded AFC setup and an improved strake location.

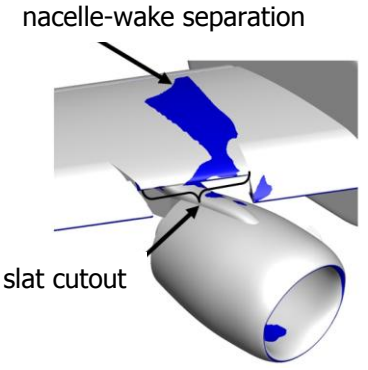

Figure 1: Nacelle-wake separation

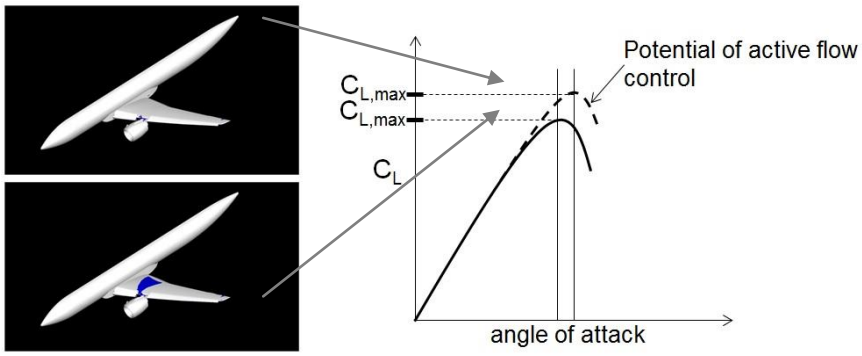

Figure 2: Potential improvement of the maximum lift coefficient due to active flow control

2 BASICS

2.1 Wind Tunnel Model

The analyzed 2.5D high-lift wind tunnel model geometry with an underwing potted throughflow nacelle is illustrated in Figure 3. The reference area is S_{ref} =16.29m^2 and the reference cord length L_{ref} =3.259m which leads to an aspect ratio of 1.62. The wing has a sweep angle of 28°. The freestream velocity is Mach number M=0.15 which results in a chord Reynolds number of Re_c=11.4x10^6. A state-of-the-art supercritical high-lift airfoil, the DLR F-15, is used, which was intensively investigated over the last decades at DLR (see Wild [10]). The model is bounded at the inboard and outboard side (as specified in Figure 4) by two side plates to reduce the effects of the small aspect ratio. The leading edge element is a slat, which has a deflection angle of 28°. The trailing edge element is a single slotted flap with a

deflection of 35° which corresponds to a landing configuration. A strake is placed on the inboard side of the nacelle.

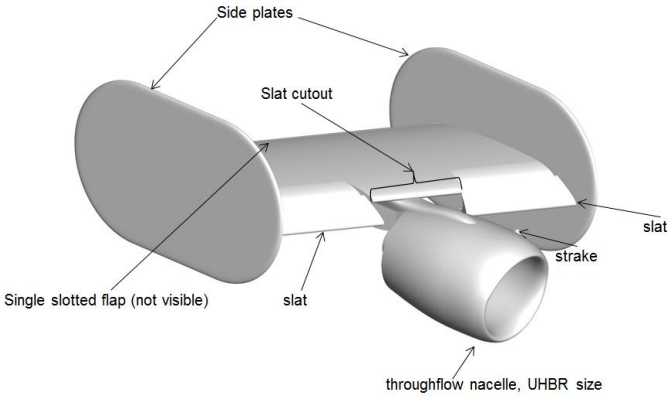

Figure 3: Wind tunnel model

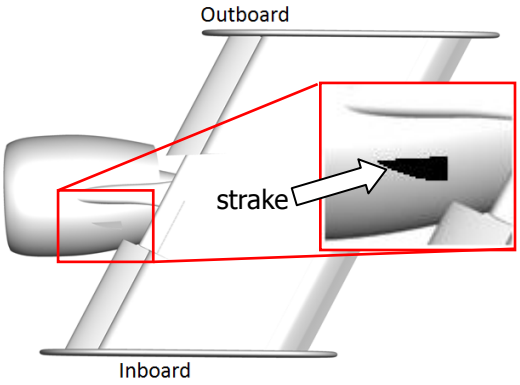

Figure 4: Top view of the wind tunnel model

The planned wind tunnel experiment will take place in the TsAGi T-101 [11] in Moscow. The scale of the wind tunnel model allows the testing of full scale active flow control systems.

2.2 Basics of Active Flow Control

Active flow control is the manipulation of the kinetic energy of the boundary layer with additional energy. It can e.g. be used to delay the transition of the boundary layer from laminar to turbulent. Another very common use is the suppression of flow separations by increasing the kinetic energy of the boundary layer which increases its resistance against adverse pressure gradients. The first to analyze this technology was Prandtl in 1904 [12]. Since then a number of different actuators were developed (see also Cattafesta [14]). Typical applications using a blowing method differentiate between a constant blowing and a time dependent blowing. For the last a common successful approach is the pulsed blowing with a square-shape signal. Constant blowing directly increases the kinetic energy of the boundary layer. The modern pulsed blowing induces longitudinal and spanwise vortices that increase the mixing of the boundary layer with the high energetic free stream flow (see Greenblatt [9]). It can be more efficient and reach the same effect as constant blowing with less required air mass flow. Overall four basic parameters are generally characterizing an unsteady blowing. The most important is the blowing momentum coefficient C_μ which describes the amount of momentum introduced into the flow. It is based on the first formulation of Poisson-Quinton [15] for steady blowing, and here is used according Brunet [16] who extended the formulation to consider unsteady actuation and is defined as

$$C_\mu = \frac{1}{DC}\frac{\overline{\dot{m}_j} U_j}{\frac{1}{2}\rho_\infty U_\infty^2 S_{ref}} \tag{1}$$

where U_j is the peak actuator outflow velocity over time, m_j the mean mass flow over time required by the actuators, S_{ref} the reference area and $\frac{1}{2}\rho_\infty U_\infty^2$. the dynamic pressure. The duty cycle DC gives the duration where the actuation is active t_{active} in relation to the total actuation cycle T.

$$DC = \frac{t_{active}}{T} \tag{2}$$

The non-dimensional frequency F^+ depends on the reference length L_{ref}, the freestream velocity U_∞ and the pulse frequency of the actuator f. Usually the number of induced structures is 2 x F^+ depending on the convectional speed of the vortexes. For the discussed case the chord length of the wind tunnel model, which is described in chapter 2.1, is used as reference length L_{ref}.

$$F^+ = \frac{f\ L_{ref}}{U_\infty} \tag{3}$$

The global velocity ratio Λ gives the relation between the jet exit velocity U_j over the freestream velocity U_∞.

$$\Lambda = \frac{U_j}{U_\infty} \tag{4}$$

2.3 Active Flow Control Setup

The followed technology path for the wind tunnel test is the pulsed jet actuation. Here every actuator consists of a pair of exit nozzles. Both blow out with a time-phase shift of 180° as sketched in Figure 5. This kind of actuation leads to a combination of dominating longitudinal and spanwise vortices.

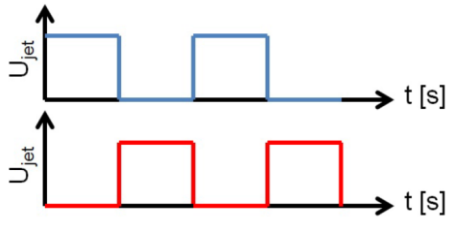

Figure 5: Exit velocity of the two blowing slots of an actuator over time

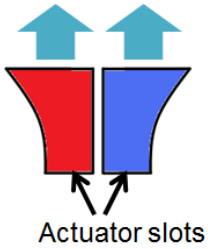

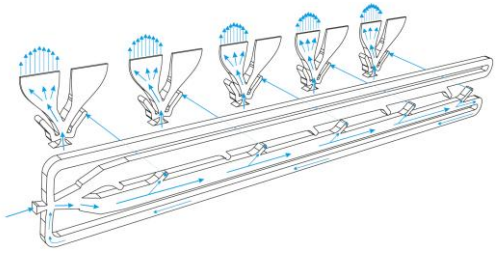

Figure 6: Used actuator concept (picture taken from [21])

The design of the physical actuators is based on Goelling and Bauer [17] and was already successfully used in wind tunnel experiments by Bauer et. al [18]. The application of the pulsed blowing through slits was intensively investigated in Germany over the last decade by Petz and Nitsche [20], Haucke and Nitsche [21], Bauer et. al [19] and later adapted to use the fluidic oscillator approach by Bauer et al. [22]. Figure 6 shows the last concept of the switching between the two slots of one actuator as used in the presented study and is further described by Meyer [23]. It is controlled by fluidic feedback loops which are based on the concept of Viets [24]. Figure 7 shows the position of the actuators on the wind tunnel model. Overall seven actuator pairs are located on the suction side of the wing at the inboard site of the slat cutout. Each slot has an exit area of 60mm x 6mm. The distance between adjacent slots is 10mm. The angle between the surface of the wing and the blow direction is 30°. The yaw angle of the blowing is parallel to the end plates.

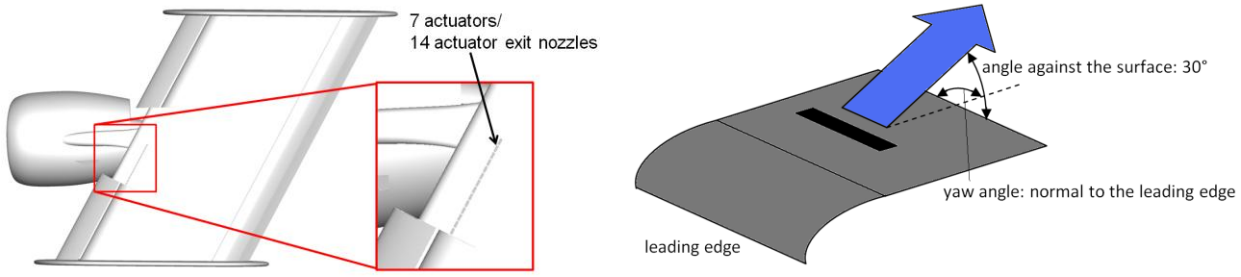

Figure 7: Location and blowing direction of the actuator slots on the suction side of the wing

2.4 Nacelle Strake Aerodynamics

The nacelle strake is a very common aerodynamic element for the improvement of the flow around the engine-wing junction at high angles of attack. The downwash of the strake vortex on the areas without leading edge elements and the increased mixing of the boundary layer with the freestream flow stabilize the boundary layer in the areas of the main wing element. Despite of the common use of nacelle strakes there are not many scientific analyses of the interaction of the strake vortex with the flow around the wing. Rudnik [2], Neitzke et al. [3], v. Geyr [4] performed detailed experimental measurements and identified the impact of inboard and outboard located strakes on the nacelle for high lift wing body aircraft configurations with under wing mounted through-flow nacelles. Zhang et al. [25] performed a numerical parameter study of the strake position which showed that the form and position of the nacelle strake has a huge impact on the suppression of the nacelle-wake separation. M. Kanazaki [26], Y. Yokokawa [27], M. Murayama et al. [28] conducted a parameter study during a wind tunnel experiment and confirmed that the position, size and form of the nacelle strake have a very large impact on the development of the separation in the wake of the engine nacelle and hence on the maximum achievable lift.

3 NUMERICAL APPROACH

The DLR in-house RANS-solver TAU [29] was used for the flow simulations. The turbulence was modelled with the one-equation Spalart-Allmaras model (see Spalart and Allmaras [30]) including a vortex correction approach according to Shur et al. [31]. All unsteady computations were performed using a dual time stepping approach. 100 time steps were used for time discretization of one actuation period. Each time step had 400 inner iterations. The computational domain was discretized with a hybrid approach using the commercial mesh generator Centaur. The surface was discretized with triangles, 38 prisms stacks are used for the spatial discretization of the boundary layer, and for the rest of the volume tetrahedron were used. Figure 8 shows the surface grid, which contains 2.2 million elements. The mesh has a total of 42 million points.

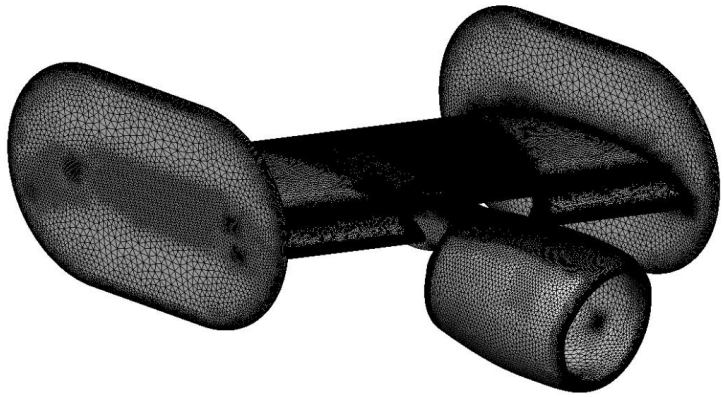

Figure 8: Surface grid

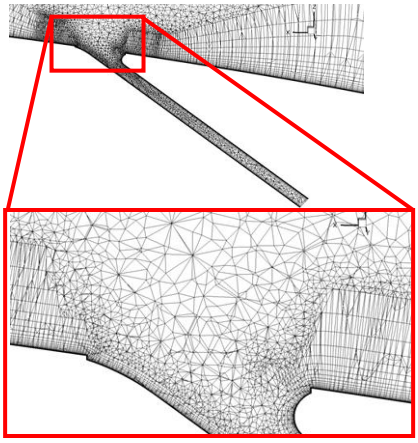

Figure 9: Details of the mesh around the actuator

The actuators are modelled based on the best practice method for flow control simulations of Ciobaca [32]: The slit-actuators are modelled as straight slits with the length of 20 times the slit width as illustrated in Figure 9. The three dimensional and largely curved form of the exit nozzle, as illustrated in Figure 6, is not modelled.

4 RESULTS

4.1 Overview over computed Cases

All presented cases in this paper were analyzed at a fixed large AoA (angle of attack), α=30°. The AoA was shown by Fricke et al. [8] to be larger than the minimum required incidence to cause a large nacelle-wake separation for the DLR-F15 swept wing with an under wing-mounted through-flow nacelle at the given wind tunnel setup. The inflow conditions are based on the environment of the wind tunnel. The free stream velocity is U_∞ = 51m/s, the air temperature T_∞=288.15K, the pressure p_∞= 101325Pa which results in the density ρ_∞ = 1.225kg/m³. The temperature of the air blown out of the actuator is T_j=288.15K, the pressure p_j= 101325Pa and the density ρ_j = 1.225kg/m³. Overall 4 cases were analyzed. The details are presented in Table 1Table 1.

Case	C_μ [%]	U_j [m/s]	$\dot{m}$ [kg/s]	Λ [-]	DC[-]	f [Hz]	F^+ [-]	AoA [°]
1	0.95	200	0.62	3.92	0.5	60	3.83	30
2	1.76	272	0.84	5.33	0.5	60	3.83	30
3	1.76	272	0.84	5.33	0.5	20	1.28	30
4	1.76	272	0.84	5.33	0.5	100	6.38	30

Table 1: Computed cases

4.2 Description of the Flow Topology

The flow field about the engine-wing junction in high-lift condition is very complex. Figure 10 shows with the help of the Λ2-criterion (see Jeong [33]) the vortices in the wake of the engine nacelle including the vortices induced by the AFC application. It is clear that this area is dominated by three longitudinal vortices: The strake vortex is emerging at the nacelle strake and is going directly over the AFC actuators.

The pylon shoulder vortex is emerging at the inboard side of the pylon and is also located directly over the actuator slots. The last dominating vortex is emerging at the slat end. It can be seen that this vortex is fragmented by the pulsed blowing of the actuators. Figure 11 shows the flow separation areas and the surface friction lines in post-stall conditions (base flow without actuation). As it can be seen two dominant local flow separation regions exist: The large corner flow separation (1) and the nacelle-wake separation (2). The flow in the whole section of the main wing element located at the inboard side of the slat cutout is separated.

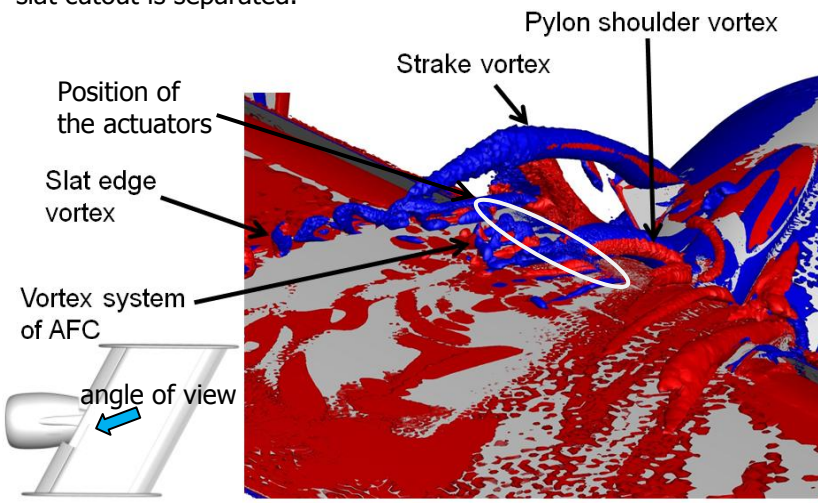

Figure 10: Vortices on the wing suction side in the wake of the nacelle, instant picture, AFC active

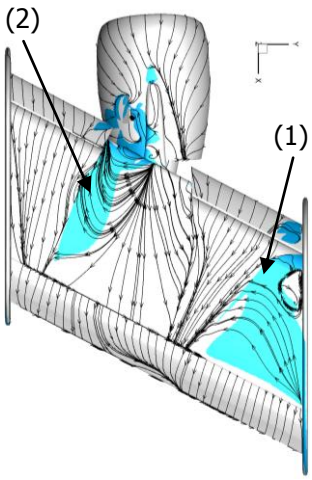

Figure 11: Surface friction lines and flow separation regions, AFC inactive

The wing stall of the wind tunnel model is triggered by the corner flow separation (1). Since the wing stall of the wind tunnel model is not triggered by the nacelle-wake separation the impact of the application of AFC is not visible in the force coefficient. Therefore the further discussion will focus on the changes of the flow topology due to the actuation.

4.3 Effects of the pulsed blowing

Figure 12 shows the surface friction lines and the flow separation areas for computation case 1 with a jet velocity of 200m/s for several instantaneous snapshots over one actuation period. The flow separation areas are identified with a negative friction coefficient C_f. Obviously the flow is separated in the wake of the nacelle over the whole actuation period. However the active blowing slots can locally reattach the flow in the flow separation area over a small area. Figure 13 shows analogue to Figure 12 the surface friction lines and the separation areas for case 2 which has an increased jet velocity of 272m/s. Opposed to case 1 the nacelle-wake separation is almost completely suppressed. Only at the inboard actuator small periodically appearing separated flow areas emerge.

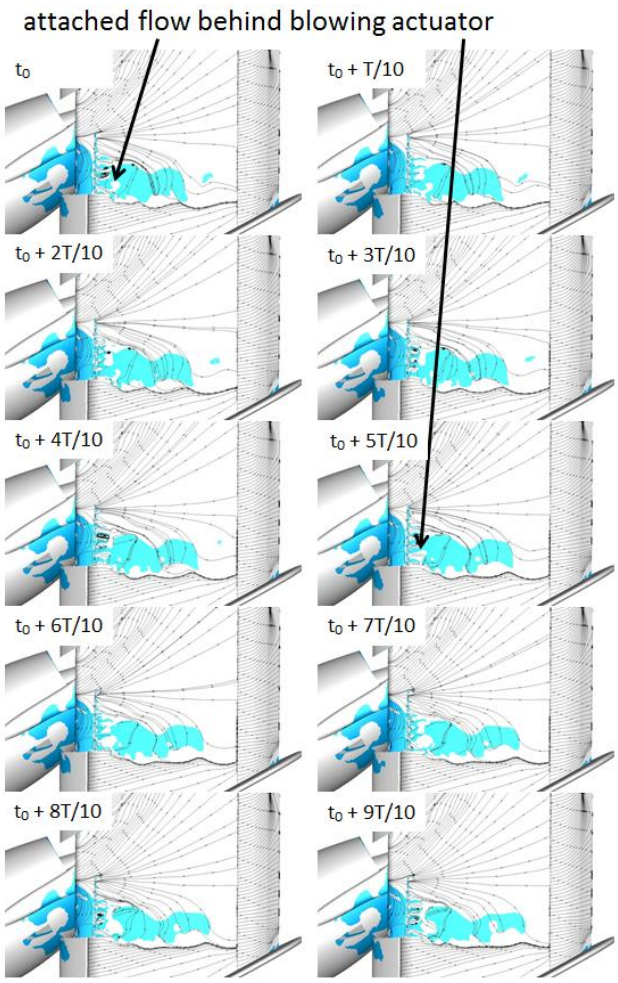

Figure 12: Surface friction lines and separated areas in blue made visible with friction coefficient C_f< 0, velocity ratio Λ=3.92, AOA=30°, M0.15 , U_j=200m/s (case 1)

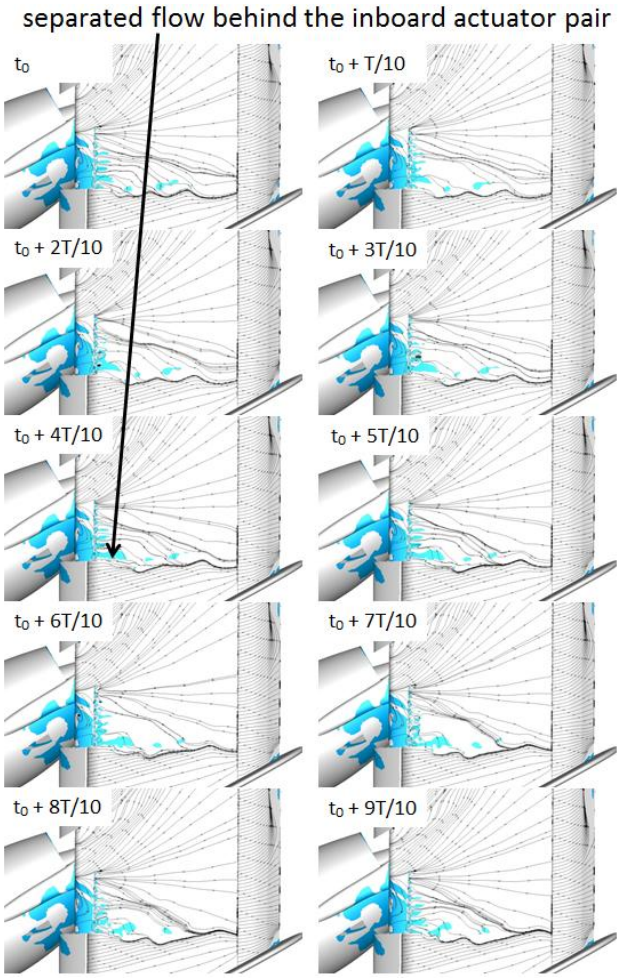

Figure 13: Surface friction lines and separated areas in blue made visible with friction coefficient C_f< 0, velocity ratio Λ=5.33, AOA=30°, M0.15 , U_j=272m/s (case 2)

Figure 14 shows a field slice with the velocity in x-direction over time for one actuation period analog to the results presented in Figure 12 and 13. For the case with a velocity ratio of Λ=3.92 corresponding to a jet velocity of 200m/s the recirculation area downstream of the actuator is visible. For Λ=5.33 with Uj=272m/s the velocity in the wake of the actuators is positive for the whole actuation cycle which is an indicator that the mixing of the boundary layer with the freestream flow is taking place.

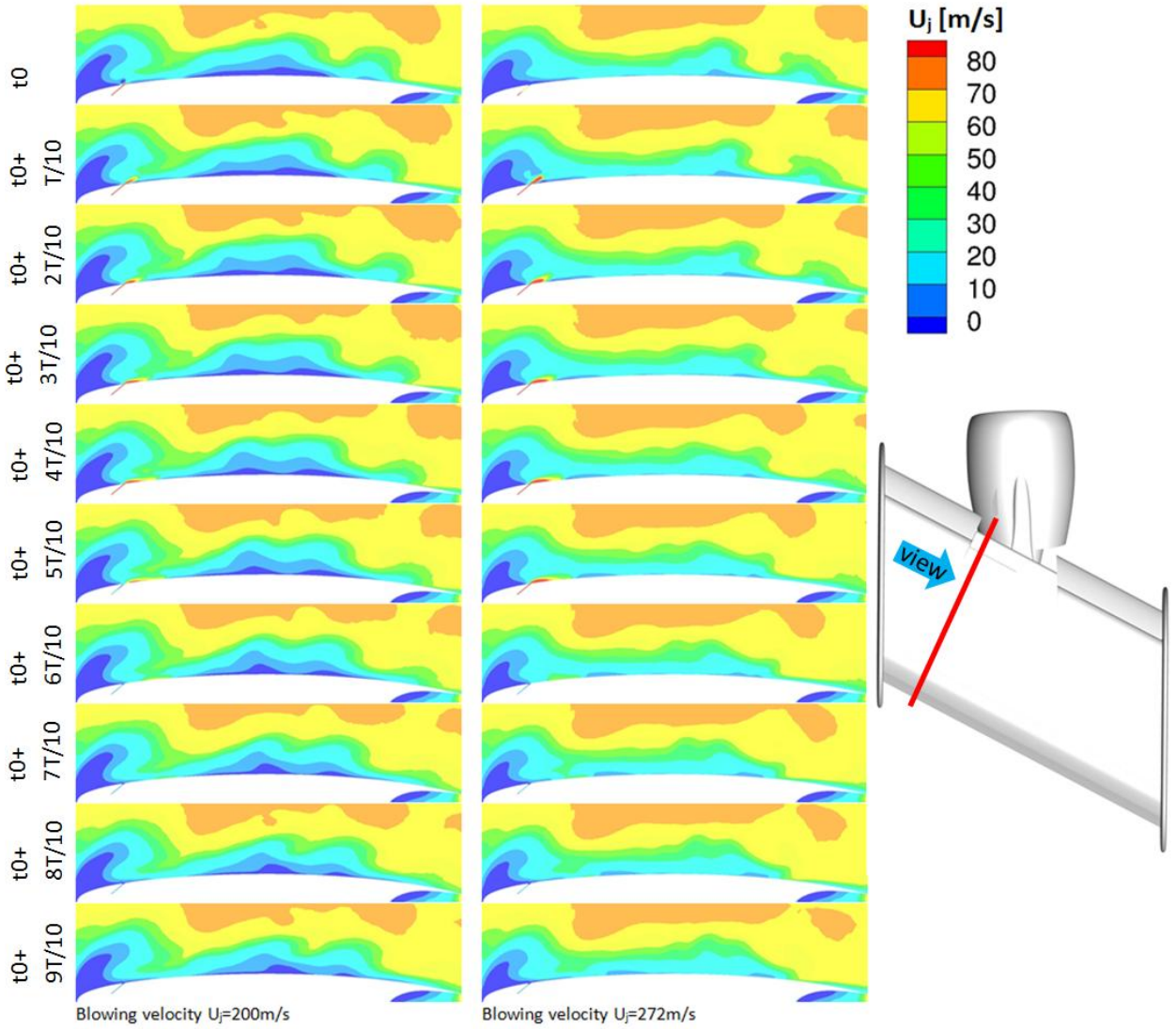

Figure 14: Cut plane with the flow velocity in x-direction for case 1 and 2.

4.4 Influence of the Pulse Frequency

Three different frequencies were investigated for a jet velocity of 272m/s: the frequency already applied for the jet velocity variation of F^+=3.83, a smaller frequency of F^+=1.28 and a larger one of F^+=6.38. The flow topology behind the nacelle on the wing does not change significantly after several calculated periods. The resulting figures with areas of negative friction coefficients, indicating separated flow, are presented in Figure 15. It can be seen that the separation downstream of the actuator is suppressed in all three cases with the differing frequencies. There is no clear difference between the cases, and in is not possible to conclude from the computed cases which would be best at preventing separation at higher angles of attack.

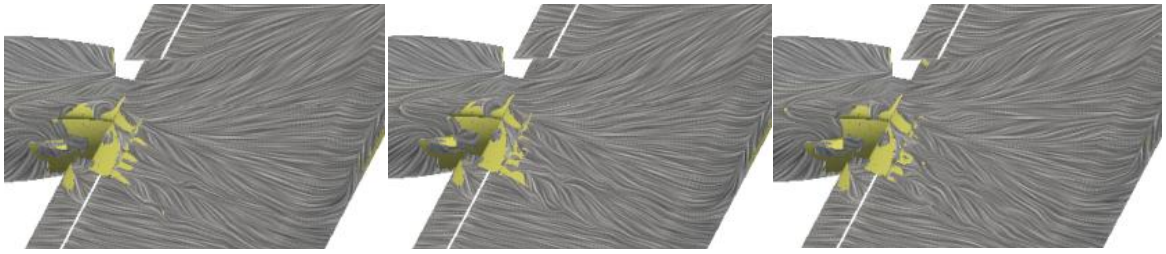

Figure 15: Surface friction lines and separated areas in yellow made visible with friction coefficient $C_f < 0$. From left to right: $F^+ = 1.28$, $F^+ = 3.83$, and $F^+ = 6.38$.

5 CONCLUSION

Numerical simulations of pulsed active flow control at the engine-wing junction of a generic full scale wind tunnel model are presented. At high angles of attack local flow separations can appear on the wing suction side of backward swept wings with underwing mounted engines in the area of the engine-wing junction. This can cause the total wing stall which reduces the maximum achievable lift and hence the overall aircraft performance. The intensity of these local flow separations depend strongly on the diameter of the nacelle of the engine. The use of nacelle strakes, large vortex generators, is currently successfully used for the suppression of the local flow separation with today's modest sized engine nacelles. It is believed that they won't be enough for future UHBR nacelles with a larger diameter. AFC is believed to be able to suppress the local flow separations at engine-wing junctions. In this paper the use of pulsed active flow control is analyzed. The working principle of the pulsed blowing is the creation of vortices that increase the mixing of the boundary layer and the free stream flow. Earlier studies have shown that the interaction between the nacelle strake and the vortices induced by the AFC is important for the functioning. In this paper a parameter study is presented. The blowing velocity and the pulse frequency were varied to study their influence on the suppression of the nacelle-wake separation. The results show that the pulsed actuation is able to suppress the flow separation on the suction side of the main wing element for a high blowing velocity. A lower blowing velocity failed to suppress the nacelle-wake separation. The variation of the pulse frequency shows the effect of low impact of F+ values of 1.28 to 6.38 on the shown ability of AFC to suppress the nacelle wake separation. The presented setup will be used in the wind tunnel test.

6 ACKNOWLEDGEMENT

The authors would like to thank all the partners in AFLoNext work package 2.1 for the great cooperation. The work described in this paper and the research leading to these results has received funding from the European Commission Seventh Framework Programme FP7/2007-2013, under grant agreement n° 604013, AFLoNext project.

7 REFERENCES

[1] Guynn M. D. et al., Refined Exploration of Turbofan Design Options for an Advanced Single-Aisle Transport. NASA/TM2011-216883, 2011

[2] R. Rudnik, "Stall Behavior of the EUROLIFT High Lift Configurations" in 46th AIAA Aerospace Sciences

Meeting and Exhibit, AIAA Paper 2008-836, 2008
[3] K.-P. Neitzke, R. Rudnik, S. Schroeder, "Low Speed Validation Tests on Engine/Airframe Integration Within the EC Project EUROLIFT II", AIAA Paper 2005-3704, 2005
[4] H. v. Geyr, N. Schade, J. W. van der Burg, P. Eliasson, S. Esquieu, "CFD Prediction of Maximum Lift Effects on Realistic High-Lift-Commercial-Aircraft-Configurations within the European Project EUROLIFT II", AIAA Paper 2007-4299, 2007
[5] C.P. van Dam, The Aerodynamic Design of Multi-Element High-Lift Systems for Transport Airplanes, Progress in Aerospace Sciences 38 (2002) 101-144, 2002
[6] M. Meyer, M. Lengers, H. Bieler, S. Fricke, J. Wild, D. Norman, "Designing and Testing Active Flow Control Systems at the Junction of Ultrahigh Bypass Ratio Engines and the Wing", Eccomas Presentation, 2014
[7] EU-project AfloNext, URL: www.AfloNext.eu
[8] S. Fricke, V. Ciobaca, J. Wild, D. Norman, "Numerical Studies of Active Flow Control applied at the Engine-Wing Junction", Symposium "Simulation of Wing and Nacelle Stall", 2014
[9] D. Greenblatt, I. Wygnaski, The Control of Flow Separation by Periodic Excitation, Progress in Aerospace Sciences, 36(7): 487-545, 2000
[10] J. Wild, Mach and Reynolds Number Dependencies of the Stall Behaviour of High-Lift Wing Sections", Journal of Aircraft, 50 (4):1202-1216 , 2013
[11] http://tsagi.com/experimental_base/wind-tunnel-t-101/, accessed on May 2015
[12] L. Prandtl, Ueber Fluessigkeitsbewegung bei sehr kleiner Reibung - Verhandlungen III, Internationaler
[13] mathematischer Kongress, Heidelberg, 1904
[14] Cattafesta III, L. N., Sheplak, M., Actuators for Active Flow Control, Annual Review of Fluid Mechanics, Vol. 43: 247-272, 2011
[15] P. Poisson-Quinton, Recherches théoretiques et éxperimentales sur le controle de couche limite, 7th Congress of Applied Mechanics, Aerospace Science and Technology, 1948
[16] Brunet, V., Dandois, J., Verbeke, C., Recent Onera Flow Control Research on High-Lift Configurations, AerospaceLab Journal, Issue 6, 2013
[17] B. Goelling, M. Bauer, Fluid actuator for producing a pulsed outlet flow in the flow around an aerodynamic body, and discharge device and aerodynamic body equipped therewith, Patent, US2012/0186682A1
[18] M. Bauer, J. Lohse, F. Haucke, and W. Nitsche, "High-Lift Performance Investigation of a Two-Element Configuration with a Two- Stage Actuator System," AIAA Journal, Vol. 52, No. 6, 2014, pp. 1307–1313.
[19] M. Bauer, I. Peltzer, W. Nitsche, B. Goelling, Active Flow Control on an Industry-Relevant Civil Aircraft Half Model, Notes on numerical Fluid Mechanics and Multidisciplinary Design, Vol. 108: 95-107, Springer Verlag, 2010
[20] R. Petz, W. Nitsche, Active Separation Control on the Flap of a two-dimensional Generic High-Lift Configuration, Journal of Aircraft, 44(3):865-874, 2007
[21] F. Haucke, W. Nitsche, "Active Separation Control on a 2D High-Lift Wing Section towards High Reynolds Number Application", AIAA Paper 2013-2514, 2013
[22] M. Bauer, T. Grund, and W. Nitsche, "Experiments on active drag reduction on a complex outer wing model," AIAA Journal, pp. 1-10, Dec. 2014
[23] M. Meyer, W. Machunze, M. Bauer, "Towards the Industrial Application of Active Flow Control in Civil Aircraft – An Active Highlift Flap", AIAA Paper 2014-2401
[24] H. Viets, Flip-Flop Jet Nozzle, AIAA Journal, 13(10): 1375-1379, 1975
[25] W. Zhang, H. Chen, Y. Zhang, S. Fu, Y. Chen, Y. Li, Tao Zhou Numerical Research of the nacelle strake on a civil jet, 28th International Congress of the Aeronautical Sciences, 2012
[26] M. Kanazaki, Y. Yokokawa, M. Murayama, et al., "Efficient Design Exploration of Nacelle Chine Installation in Wind Tunnel Testing", AIAA Paper 2008-155, 2008
[27] Y. Yokokawa, M. Murayama, M. Kanazaki, et al., "Investigation and Improvement of High-Lift Aerodynamic Performances in Lowspeed Wind Tunnel Testing", AIAA Paper 2008-350, 2008
[28] Y. Yokokawa, M. Murayama, H. Uchida, et al., "Aerodynamic Influence of a Half-span Model Installation

for High-Lift Configuration Experiment", AIAA Paper 2010-684, 2010
[29] Technical Documentation of the DLR TAU-Code Release 2013.1.0, 2013
[30] P.R. Spalart, S.R. Allmaras, "A One-Equation Turbulence Model for Aerodynamic Flows", AIAA Paper 91-0439, 1992
[31] M. L. Shur, M. K. Strelets, A. K. Travin, P. R. Spalart, Turbulence Modeling in Rotating and Curved Channels: Assessing the Spalart-Shur Correction. AIAA Journal, 38(5):784–792,2000
[32] V. Ciobaca, Validation of Numerical Simulations for Separation Control on High-Lift Configuration, DLR IB-1014-11, Phd-thesis, Technical University Berlin, 2014
[33] J. Jeong, F. Hussain, On the Identification of a Vortex, Journal of Fluid Mechanics, 285:69-94, 1995